Evaluation of External Electromagnetic Fields Generated by A Multi-Phase Underground Cable Based on Transmission Line Approach

H. Xue and J. Mahseredjian

***Abstract*—Recently developed extended transmission line (TL) approach and generalized formulas of external electromagnetic (EM) fields generated from a multiphase underground cable are reviewed and summarized in this paper. The lateral external EM field components of a three-phase underground cable with different arrangements are evaluated by classical and extended TL approaches. Two phase and single-phase energizations are applied to the cable. The characteristics of external EM fields at different field observation points are calculated.**

***Keywords*: Underground cables, external electromagnetic fields, transmission line approach, numerical calculations.**

I. Introduction

EXTERNAL Electromagnetic (EM) fields in the lossy earth generated by a single phase underground cable are investigated in [1]-[4]. In [1]-[4], the accurate formulas of EM fields produced from the single phase underground cable are derived. The EM field components of the single-phase cable are calculated based on approximate formulas of transmission line (TL) approach, and the results are also validated by the exact analytical solutions.

Recently, an extended TL approach has been developed in [5]-[8]. It shows a significant influence on transient simulations of a cross-bonded underground cable, that is, the visible effects of earth-return parameters of the cable are observed. The earth-return impedance and admittance formulas proposed in [5] are based on the analytical solutions of complete EM field components. Next, the extended TL approach has been adopted into the study of external EM fields produced from a multi-phase underground cable [9]. Also, the generalized earth-return impedance and admittance formulas used in the extended TL approach are thoroughly compared and validated with Numerical Electromagnetic Code 4.2 [10] in [9]. Thus, the effectiveness of extended TL approach has been further proved.

In [9], a series of numerical calculations of external EM field based on Phases A - B (inter-phase) and Phase - B (earth-return) energizations on a three-phase underground cable has been performed. The modal propagation constants, the lateral profiles of external EM field components, the influence of earth resistivity and permittivity on external EM field components, the shielding effect of cables and the phase current in the cable at high frequencies are calculated and analyzed. Also, the differences of EM field components calculated by the extended and classical TL approaches are made clear. However, the investigations conducted in [9] are only based on a flat arrangement of the cable.

Considering above facts, the previous investigations which include the extended TL approach and external EM field expressions of a multi-phase underground cable in [5]-[9] are summarized in Section II. In Section III, three different arrangements of a three-phase underground cable are adopted into calculations of external EM field components. The influences of classical and extended TL approaches on the results of external EM fields are further examined and studied based on different arrangements of cable.

II. Theoretical Backgrounds

The recently proposed classical / extended TL approaches, vectors of external EM fields generated from a multi-phase underground cable and energizations are reviewed and summarized in this section.

A. Calculation of Propagation Constants by TL Approaches

As discussed in [5], the TL approach is characterized by the extended TL approach and classical TL approach. For the extended TL approach, the generalized formulas of series impedance and shunt admittance of a multi-phase underground cable are given by

$$\mathbf{Z} = \mathbf{Z_i} + \mathbf{Z_e} \tag{1}$$

$$\mathbf{Y} = j\omega\mathbf{P}^{-1} \tag{2}$$

where $\mathbf{Z_i}$ is the internal impedance matrix of the cable and consists of the conductor and the insulator impedances [11], $\mathbf{Z_e}$ is the earth-return impedance matrix of the cable [5] and the potential coefficient matrix $\mathbf{P}$ is defined as

$$\mathbf{P} = \mathbf{P_i} + \mathbf{P_e} \tag{3}$$

where $\mathbf{P_i}$ and $\mathbf{P_e}$ are the internal and earth-return potential coefficient matrices of the cable [11], [12].

If earth permittivity and $\mathbf{P_e} = 0$ are assumed in (1) and (2), then it is defined as classical TL approach which is the same as the earth-return impedance formula derived in [13] and

H. Xue is with the Global Energy Interconnection Development and Cooperation Organization, Global Energy Interconnection Group Co. Ltd and Polytechnique Montréal, Ethiopia, China and Canada (e-mail: haoyan.xue@polymtl.ca).
J. Mahseredjian is with Polytechnique Montréal, Canada (e-mail: jean.mahseredjian@polymtl.ca).

Paper submitted to the International Conference on Power Systems Transients (IPST2021) in Belo Horizonte, Brazil June 6-10, 2021.

insulator potential coefficient used in original Cable Constants [14].

The unknown modal propagation constants and current/ voltage transformation matrices can be calculated by solving the eigenvalues and eigenvectors of the product of (1) and (2) without any difficulties.

B. External Electromagnetic Characteristics of Underground Cable

The following generalized formulas of external EM fields generated from a multi-phase underground cable have been derived and proposed in [9].

$$\left.\begin{aligned}\mathbf{E}_1(x,y,z)&=\mathbf{\Phi}_1(y,z)\mathbf{i}(x)\\ \mathbf{H}_1(x,y,z)&=\mathbf{\Upsilon}_1(y,z)\mathbf{i}(x)\end{aligned}\right\} \tag{4}$$

where $\mathbf{E}_1(x,y,z)$ and $\mathbf{H}_1(x,y,z)$ are an 3×1 EM field vectors, $\mathbf{\Phi}_1(y,z)$ and $\mathbf{\Upsilon}_1(y,z)$ are $3\times N$ modal current to EM field operator's matrices [9], and $\mathbf{i}(x)$ is an $N\times1$ modal current vector.

The modal current vector of generated EM field components in (4) can be further expressed by

$$\mathbf{i}(x)=\mathbf{B}^{-1}\mathbf{I}(x) \tag{5}$$

where $\mathbf{I}(x)$ is an $N\times1$ current vector in phase domain and $\mathbf{B}$ is an $N\times N$ current transformation matrix.

Based on the assumption of unidirectional propagation of voltage and current waves, $\mathbf{I}(x)$ in (5) using the TL approach can be represented by

$$\mathbf{I}(x)=\mathbf{Y}_0\mathbf{A}\boldsymbol{\zeta}(x)\mathbf{A}^{-1}\mathbf{V_f} \tag{6}$$

where $\mathbf{Y}_0$ is an $N\times N$ characteristic admittance matrix of the cable system in phase domain, $\mathbf{A}$ is an $N\times N$ voltage transformation matrix, $\boldsymbol{\zeta}(x)$ is an $N\times N$ reflection free transition diagonal matrix, $\mathbf{V_f}$ is a known $N\times1$ voltage source vector at $x=0$ and

$$\mathbf{A}=\left(\mathbf{B}^T\right)^{-1} \tag{7}$$

$$\boldsymbol{\zeta}(x)=\begin{bmatrix}e^{-jk_1x} & & \\ & \ddots & \\ & & e^{-jk_Nx}\end{bmatrix} \tag{8}$$

Next, the equation (4) can be re-written by adopting (5), and it gives

$$\left.\begin{aligned}\mathbf{E}_1(x,y,z)&=\mathbf{\Phi}_1(y,z)\mathbf{B}^{-1}\mathbf{Y}_0\mathbf{A}\boldsymbol{\zeta}(x)\mathbf{A}^{-1}\mathbf{V_f}\\ \mathbf{H}_1(x,y,z)&=\mathbf{\Upsilon}_1(y,z)\mathbf{B}^{-1}\mathbf{Y}_0\mathbf{A}\boldsymbol{\zeta}(x)\mathbf{A}^{-1}\mathbf{V_f}\end{aligned}\right\} \tag{9}$$

The matrix expression of (9) defines the generated EM field of a multi-phase underground cable system in a lossy earth as a function of the known voltage $\mathbf{V_f}$.

C. Energizations Adopted into Calculations

Fig. 1 illustrates a three phase cable system with horizontal, vertical and trefoil arrangements, where the cable parameters are adopted from [15]. The outer and inner radii are $r_2=1.2$ and $r_1=1$ cm. The resistivity of core is $\rho_c=1.68\times10^{-8}\,\Omega$m. The relative permittivity of insulating jacket is $\varepsilon_{i1}=3$. The external EM field components using three different arrangements of cable system are investigated based on the extended TL and classical TL approaches.

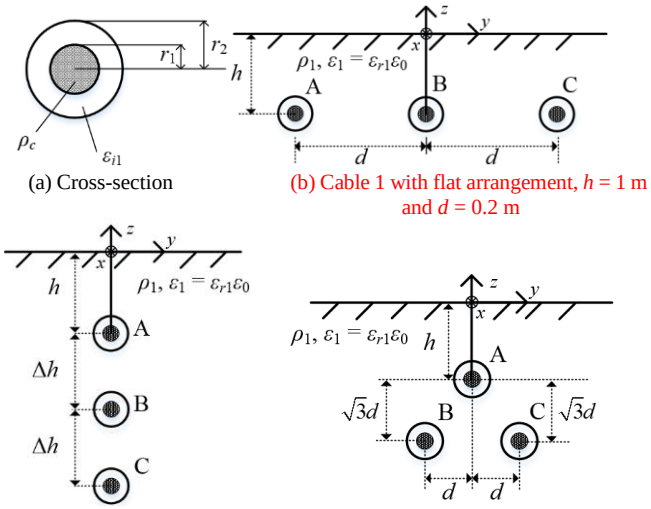

(a) Cross-section

(b) Cable 1 with flat arrangement, h = 1 m and d = 0.2 m

(c) Cable 2 with vertical arrangement, h = 1 m and Δh = 0.2 m

(d) Cable 3 with trefoil arrangement, h = 1 m and d = 0.1 m

Fig. 1 Configuration and arrangements of cables.

The following two energizations applied to the cable shown in Fig. 1 are considered in the calculations of external EM field components. The source voltage is applied at the cable sending end ($x=0$). The external EM field components (E_x, E_y, E_z, H_x, H_y and H_z) are calculated at the different positions in the earth.

1) Phases A - B energization

$\mathbf{V_f}$ in (9) is defined by the following expression for the Phases *A* - *B* energization.

$$V_{fA}=10\text{ kV},\quad V_{fB}=-10\text{ kV},\quad V_{fC}=0\text{ kV} \tag{10}$$

where V_{fA}, V_{fB} and V_{fC} are voltages applied in phases *A*, *B* and *C*, and refer to the zero potential level.

The Phases A - B energization involves a mixed mode of earth-return and inter-phase effects on the external EM field components.

2) Phase - B energization

For the Phase - *B* energization, $\mathbf{V_f}$ in (9) has

$$V_{fA}=0\text{ kV},\quad V_{fB}=10\text{ kV},\quad V_{fC}=0\text{ kV} \tag{11}$$

The Phase - B energization mainly excites the earth-return effect on the external EM field components.

III. Numerical Calculations

The different cables and energizations are used in the calculations of EM field components in this section. The earth resistivity ρ_1 is set to 100Ωm and earth relative permittivity ε_{r1} is assumed to be 1. Also, the influence of earth permittivity on results of earth-return impedance, admittance and external EM field components are minor, as observed in [5] and [9].

Furthermore, if the metallic sheath should be considered in the internal structure of cable, additional boundary conditions should be implemented into formulations of (4) based on similar approaches shown and discussed in [16], [17].

A. Horizontal Arrangement

Fig. 2 shows the calculated modal propagation constants of Cable 1 in Fig. 1 by adopting the extended and classical TL approaches. It is clear in the figure that the modal attenuation constants calculated by the extended TL approach, particularly for the inter-phase modes, increase significantly as frequency increases. Also, a significant difference is observed for the modal phase velocities evaluated by the two approaches above several hundreds of kHz. The visible differences of the modal propagation constants calculated by the two TL approaches are caused by the earth-return admittance [5].

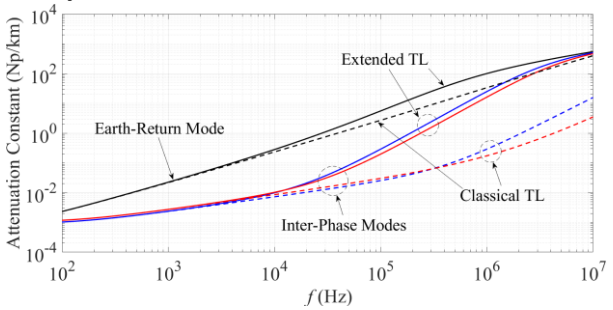

(a) Modal attenuation constants

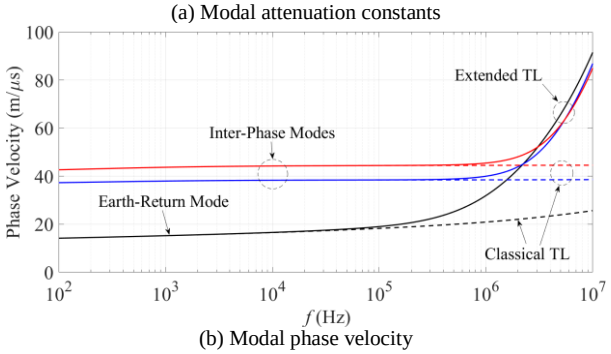

(b) Modal phase velocity

Fig. 2 Modal propagation constants evaluated by the extended and classical TL approaches with ρ_1 = 100 Ωm and ε_{r1} = 1.

Fig. 3 shows the near-field profiles of the amplitudes of lateral external EM field components calculated at 1 MHz for the Phases A - B energization. The observation point of the field is set to the position below the cable with $z = -1.5$ m.

It is clear that the external EM field components decrease smoothly as the lateral distance increases. At the frequency of 1 MHz, the external EM field components evaluated by the classical TL approach shows a significant difference to the results obtained by the extended TL approach. This phenomenon is caused by transition of the earth characteristic which is inductive initially in the low frequency region, and becomes capacitive in the high frequency region due to the effect of the earth-return admittance.

Also, it shows that the external EM field components are non-symmetrically distributed in respect of the center of arrangement of Cable 1.

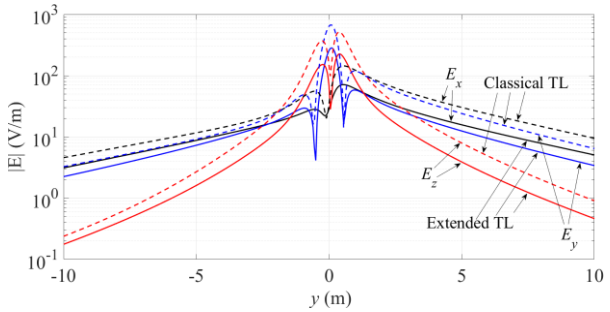

(a) Electric field components

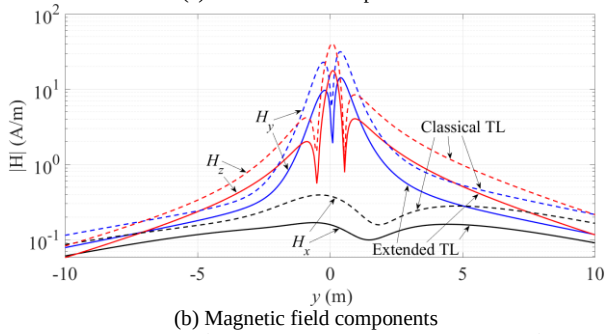

(b) Magnetic field components

Fig. 3 Lateral external EM field components calculated at 1 MHz for Phases A - B energization, x = 35 m, z = -1.5 m, ρ_1 = 100 Ωm and ε_{r1} = 1.

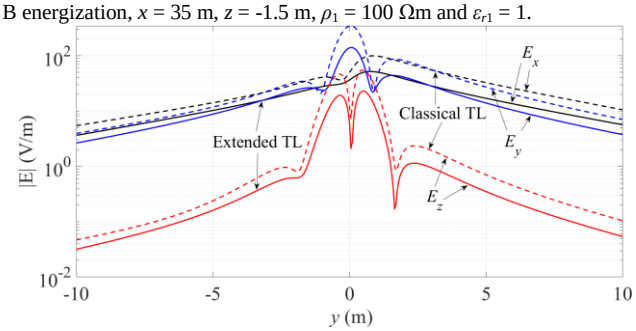

(a) Electric field components

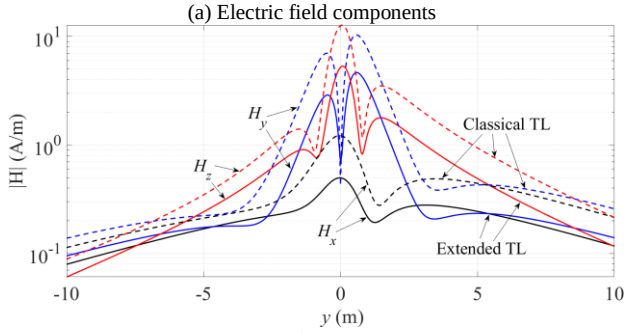

(b) Magnetic field components

Fig. 4 Lateral external EM field components calculated at 1 MHz for Phases A - B energization, x = 35 m, z = -0.1 m, ρ_1 = 100 Ωm and ε_{r1} = 1.

The external EM fields calculated nearby the earth surface at $z = -0.1$ m using the same conditions of Fig. 3 are illustrated in Fig. 4. Also, the significant effect of earth-return admittance on external EM fields is observed in the calculations. It should be noted that the external EM fields are not sufficiently attenuated since the distance between the cable and the earth surface is small.

Fig. 5 shows the calculated external EM field components as a function of the frequency. It is clear that no significant difference is observed between the results calculated by the extended and the classical TL approaches below 100 kHz. It matches with the general conclusion that the classical TL

approach is applicable to the underground cables up to a few hundreds of kHz [12]. Above 200 kHz, the external EM field components evaluated by the extended TL approach decrease rapidly.

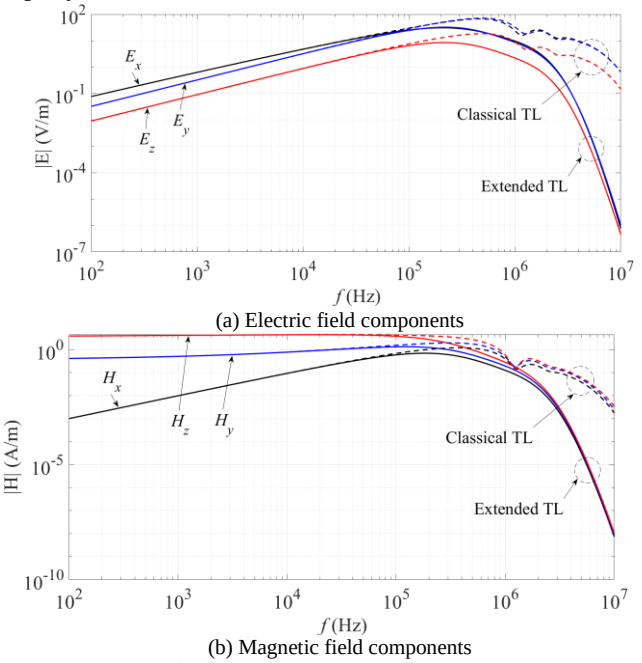

(a) Electric field components

(b) Magnetic field components

Fig. 5 External EM field components calculated at x = 35 m, y = 5 m and z = -1.5 m for Phases B energization, ρ_1 = 100 Ωm and ε_{r1} = 1.

B. Vertical Arrangement

As shown in Fig. 6, the modal propagation constants of Cable 2 using the extended and classical TL approaches are calculated.

Similar characteristics of modal attenuation constants and phase velocities calculated by the extended TL approach shown in Fig. 2 are also observed in Fig. 6, for example the results of inter-phase and earth-return modes increase obviously as frequency increases.

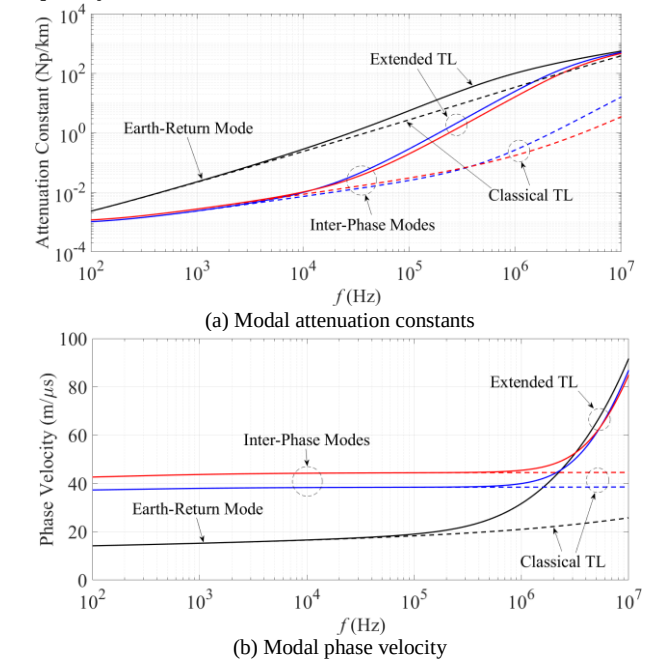

(a) Modal attenuation constants

(b) Modal phase velocity

Fig. 6 Modal propagation constants evaluated by the extended and classical TL approaches with ρ_1 = 100 Ωm and ε_{r1} = 1.

Fig. 7 illustrates the amplitudes of lateral external EM field components calculated at 1 MHz due to Phases A - B energization. The Cable 2 is adopted into the calculations.

Again, the external EM field components decrease smoothly as the lateral distance increases. The results calculated by the extended TL approach shows an important difference in comparison to the result evaluated by the classical TL approach.

Also, it is clear that the external EM field components have symmetrical distributions in respect of the center of arrangement of Cable 2.

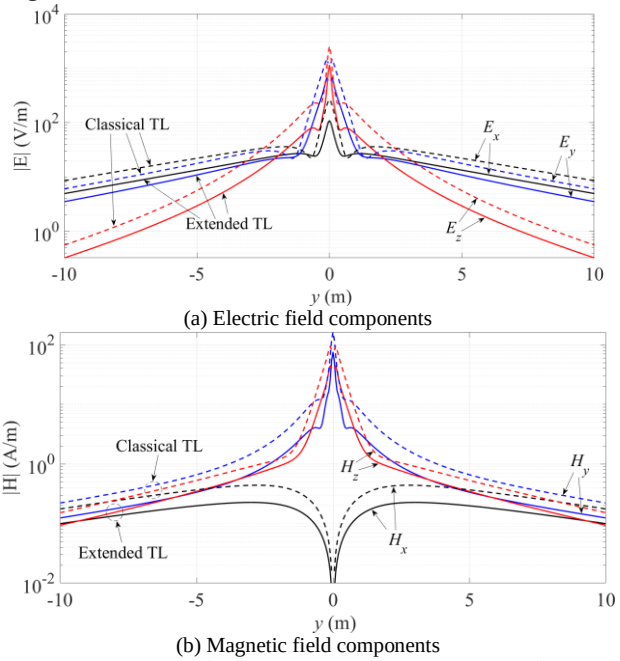

(a) Electric field components

(b) Magnetic field components

Fig. 7 Lateral external EM field components calculated at 1 MHz for Phases A - B energization, x = 35 m, z = -1.5 m, ρ_1 = 100 Ωm and ε_{r1} = 1.

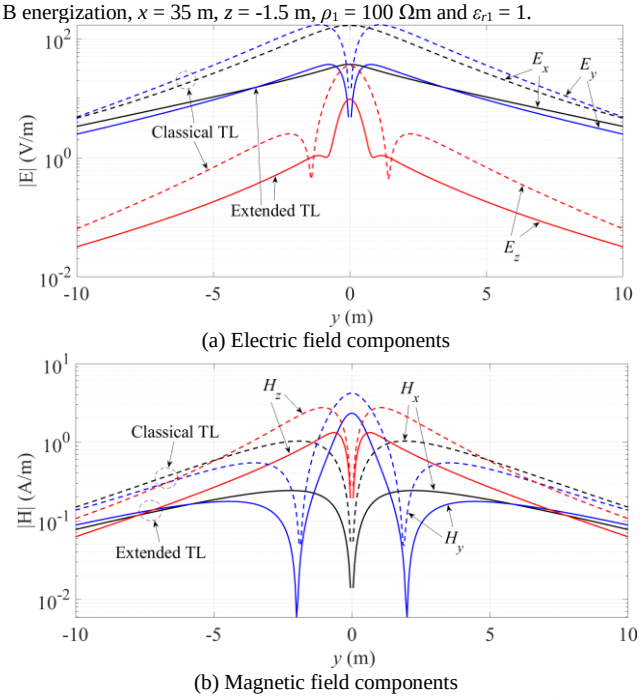

(a) Electric field components

(b) Magnetic field components

Fig. 8 Lateral external EM field components calculated at 1 MHz for Phases A - B energization, x = 35 m, z = -0.1 m, ρ_1 = 100 Ωm and ε_{r1} = 1.

Fig. 8 shows the external EM field components evaluated

nearby the earth surface with $z = -0.1$ m. In comparison to the results calculated at the position of $z = -1.5$ m, similar damping effects of external EM field components along lateral distances are observed nearby the earth surface. Also the external EM field components have not been effectively attenuated nearby the earth surface as theoretically predicted in [5].

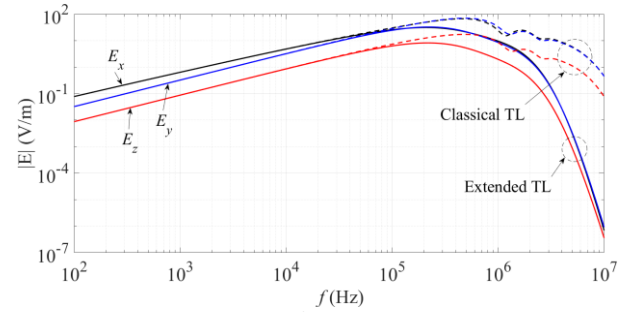

(a) Electric field components

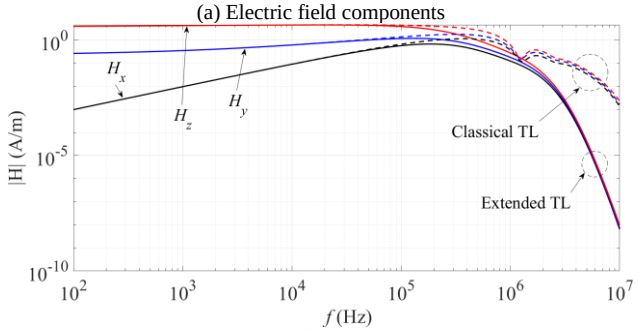

(b) Magnetic field components

Fig. 9 External EM field components calculated at x = 35 m, y = 5 m and z = -1.5 m for Phases B energization, ρ_1 = 100 Ωm and ε_{r1} = 1.

As shown in Fig. 9, no significant difference is observed between the results calculated by the extended and the classical TL approaches below 100 kHz. Also, the characteristics of external EM fields are similar to the results observed for Cable 1.

C. Trefoil Arrangement

The modal propagation constants using Cable 3 are calculated based on the extended and classical TL approaches, and the results are shown in Fig. 10.

Again, the similar characteristics of modal propagation constants shown in Fig. 2 and Fig. 6 are observed in Fig. 10. Due to trefoil arrangement of cable, the earth-return mode is nearly overlapped with an inter-phase mode.

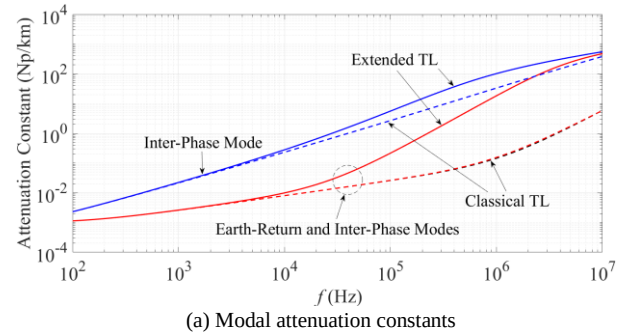

(a) Modal attenuation constants

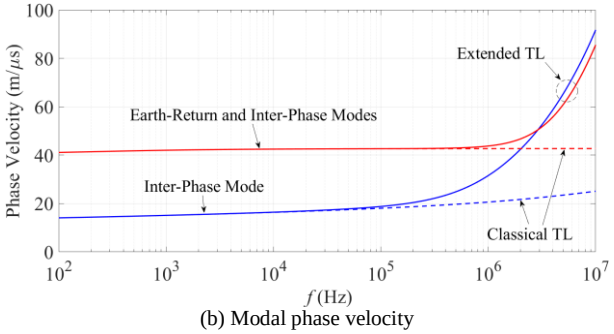

(b) Modal phase velocity

Fig. 10 Modal propagation constants evaluated by the extended and classical TL approaches with ρ_1 = 100 Ωm and ε_{r1} = 1.

Fig. 11 and Fig. 12 illustrate the amplitudes of lateral external EM field components calculated at 1 MHz due to Phases A - B energization. The observation points are selected below the cable and nearby the earth surface, respectively.

The external EM field components evaluated at two different positions show more non-symmetrical characteristics in respect of the center of arrangement of Cable 3 in comparison to calculations by Cable 1 and Cable 2.

As shown in Fig. 13, no significant difference is observed between the results calculated by the extended and classical TL approaches below 100 kHz. Also, the characteristics of external EM fields are similar to the results observed for Cable 1 and Cable 2.

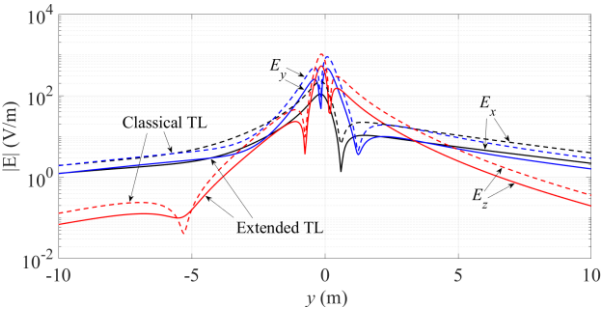

(a) Electric field components

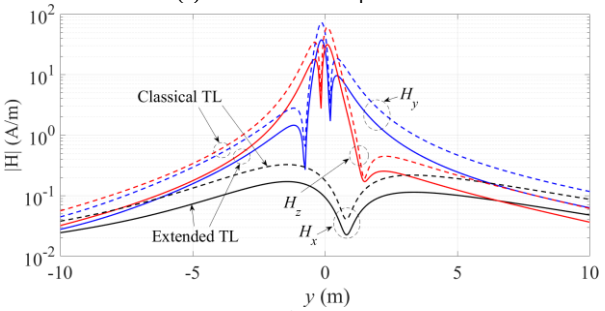

(b) Magnetic field components

Fig. 11 Lateral external EM field components calculated at 1 MHz for Phases A - B energization, x = 35 m, z = -1.5 m, ρ_1 = 100 Ωm and ε_{r1} = 1.

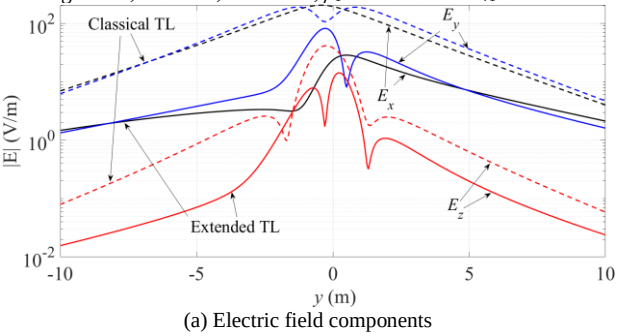

(a) Electric field components

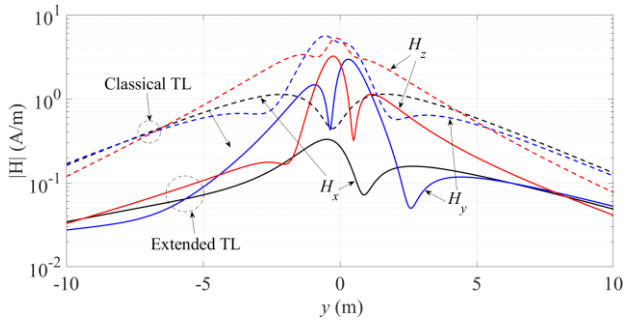

(b) Magnetic field components

Fig. 12 Lateral external EM field components calculated at 1 MHz for Phases A - B energization, x = 35 m, z = -0.1 m, ρ_1 = 100 Ωm and ε_{r1} = 1.

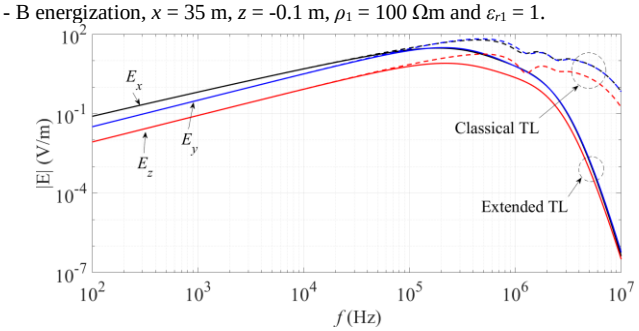

(a) Electric field components

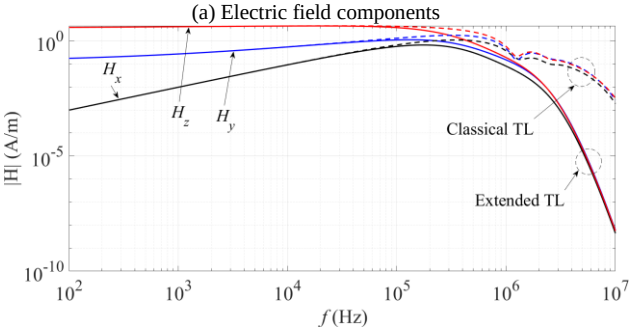

(b) Magnetic field components

Fig. 13 External EM field components calculated at x = 35 m, y = 5 m and z = -1.5 m for Phases B energization, ρ_1 = 100 Ωm and ε_{r1} = 1.

D. Discussions

In this section, the modal propagation constants calculated by classical and extended TL approaches based on three different cable arrangements are presented. The influences of cable arrangement on modal propagation constants are minor, as observed in Fig. 2, Fig. 6 and Fig. 10.

Moreover, the lateral external EM field components calculated using Cable 1 and Cable 3 show non-symmetrical distributions in respect of cable configuration due to a non-symmetrical energization. However, the Cable 2 produces symmetrical EM field components by adopting the same energization, and the reason comes from the symmetrical configurations of Phase A and Phase B. Also, the amplitudes of EM field components observed near the earth surface are lower than the results below the cables.

The extended TL approach has significant influences on external EM fields evaluated at the point x = 35 m, y = 5 m and z = -1.5 m above several hundreds of kHz.

IV. Conclusions

This paper has reviewed and summarized the recently developed extended TL approach and generalized formulation of external EM field components generated from a multi-phase underground cable based on complete field solutions. By adopting the classical TL approach and extended TL approach into the formulas of external EM fields, the TL approach based modal propagation constants and lateral external EM field components produced by a three phase underground cable are calculated and investigated. The influences of cable arrangements, i.e. flat, vertical and trefoil, on external EM fields are also studied.

Due to the influence of earth-return admittance, the modal propagation constants calculated by the extended TL approach show a significant difference to those evaluated by the classical TL approach. A complex characteristic of the external EM field distribution under Phases A - B energization is observed nearby the cable due to the non-symmetrical energization. Furthermore, a significant effect of earth-return admittance has been observed on the external EM fields produced by a multi-phase underground cable.

V. References

[1] J. R. Wait, "Electromagnetic wave propagation along a buried insulated wire," *Can J. Phys*, vol. 50, pp. 2402-2409, 1972.

[2] J. R. Wait, "Excitation of currents on a buried insulated cable," *J. Appl. phys*, vol. 49, pp. 876-880, 1978.

[3] G. Bridges, "Fields generated by bare and insulated cables buried in a lossy half-space," *IEEE Trans. Geoscience and Remote Sensing*, vol. 30, pp. 140-146, 1992.

[4] G. Bridges, "Transient plane wave coupling to bare and insulated cables buried in a lossy half-space," *IEEE Trans. Electromag. Compat*, vol. 37, pp. 62-70, 1995.

[5] H. Xue, A. Ametani, J. Mahseredjian and I. Kocar, "Generalized formulation of earth-return impedance / admittance and surge analysis on underground cables," *IEEE Trans. Power Delivery*, vol. 33, no.6, pp.2654-2663, 2018.

[6] H. Xue, A. Ametani and J. Mahseredjian, "Complete electromagnetic earth-return parameters on multi-phase underground cables Part 1: Theory," *IEEJ Technical Meeting on High Voltage Engineering*, Japan, 2018.

[7] H. Xue, A. Ametani and J. Mahseredjian, "Complete electromagnetic earth-return parameters on multi-phase underground cables Part 2: Calculation examples," *IEEJ Technical Meeting on High Voltage Engineering*, Japan, 2018.

[8] H. Xue, A. Ametani, J. Mahseredjian, Y. Baba and F. Rachidi, "Frequency response of electric and magnetic fields of overhead conductors with particular reference to axial electric field," *IEEE Trans. Electromagn. Compat.*, vol. 60, pp. 2029-2032, 2018.

[9] H. Xue, A. Ametani, and K. Yamamoto, "Theoretical and NEC calculations of electromagnetic fields generated from a multi-phase underground cable," *IEEE Trans. Power Delivery*, 10.1109/TPWRD.2020.3005521, 2020.

[10] G. J. Burke, *Numerical Electromagnetics Code - NEC - 4.2 Method of Moments Part I: User's Manual*, LLNL-SM-490875, 2011.

[11] A. Ametani, "A general formulation of impedance and admittance of cables," *IEEE Trans. PAS*, vol. PAS-99, pp. 902-910, 1980.

[12] A. Ametani, T. Ohno and N. Nagaoka, *Cable System Transients: Theory, Modeling and Simulation*, Wiley-IEEE Press, 2015.

[13] F. Pollaczek, "Uber das feld einer unendlich langen wechselstrom durchlossenen einfachleitung," *E.N.T*, vol. 3, pp. 339-359, 1926.

[14] A. Ametani, *Cable Constants*, Bonneville Power Administration, 1976.

[15] E. Petrache, F. Rachidi, M. Paolone, C. Nucci, V. A. Rakov, and M. A. Uman, "Lightning-induced voltages on buried cables - Part I: Theory, " *IEEE Trans. Electromagn. Compat.*, vol. 47, pp. 498-508, 2005.

[16] V. Malo Machado and J. F. Borges da Silva, "Series-impedance of underground cable systems," *IEEE Trans. Power Delivery*, vol. 3, no. 4, pp.1334-1340, 1988.

[17] V. Malo Machado and J. F. Borges da Silva, "Series-impedance of underground transmission systems," *IEEE Trans. Power Delivery*, vol. 3, no. 2, pp.417-424, 1988.